A Global View of Molecule-forming Clouds in the Galaxy

S. J. Gibson[1], W. S. Howard[1,2], C. S. Jolly[1,3], J. H. Newton[1,4], A. C. Bell[1,5], M. E. Spraggs[1,3], J. M. Hughes[1,3], A. M. Tagliaboschi[1], C. M. Brunt[6], A. R. Taylor[7,8], J. M. Stil[8], T. Dame[9], & IGPS Consortium

[1]Western Kentucky U., [2]Union U., [3]C. M. Gatton Acad.,[4]McMaster U., [5]U. Tokyo, [6]Exeter U., [7]U. Calgary, [8]U. Cape Town, [9]Harvard-CfA

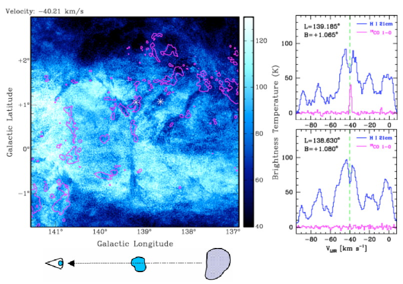

Figure 1. H I self-absorption (HISA) against warmer background H I emission (sketch) arises from atomic gas that is too cold to explain easily if it is outside molecular clouds (Wolfire et al. 2003), and yet HISA shadows often appear separate from CO emission, particularly in the outer Galaxy (Gibson et al. 2000; Gibson 2010). The panels above show CGPS H I (blue; Taylor et al. 2003) and OGS ^{12}CO 1-0 (magenta; Heyer et al. 1998). These clouds are ~ 2 kpc away in the Perseus arm, where they may be forming H_2 and CO downstream of the spiral shock before they become dense enough to form new stars (Gibson et al. 2005a).

Overview

The gas in galactic disks occurs in a wide range of temperatures and densities, most of which are unsuitable for star formation. Somehow, diffuse atomic clouds are collected into colder, denser molecular clouds that can collapse under their own gravity. Molecular condensation is not directly observable, but it most likely arises in cold, quiescent pockets of atomic hydrogen (H I) gas, which over time will form molecular hydrogen (H_2) followed by more observable molecular species. We have mapped cold 21cm line H I self-absorption (HISA) over more than 90% of the Milky Way's disk at arcminute resolution with several Galactic plane synthesis surveys. To probe the formation of H_2 clouds, we have made a detailed comparison of our HISA distribution with available CO J=1-0 line emission surveys. We find that few HISA features in the outer Galaxy have CO at the same position and velocity, while most inner-Galaxy HISA features have overlapping CO. But many of the latter apparent HISA-CO associations may only be chance superpositions, in which case the majority of inner-Galaxy HISA is also CO-free. Since standard equilibrium cloud models cannot explain the very cold H I in many HISA features without molecules being present, these clouds may instead have significant CO-dark H_2 (e.g., Wolfire et al. 2010). Many of them are found downstream of spiral shocks where H_2 formation might occur, with CO formation taking more time.

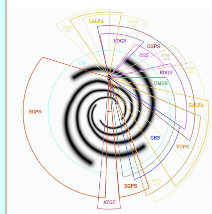

Figure 2. Galactic disk coverage of H I and CO surveys used in this study; see **Table 1** for details. GALFA data are not yet included. The spiral arm model is adapted from Taylor & Cordes (1993).

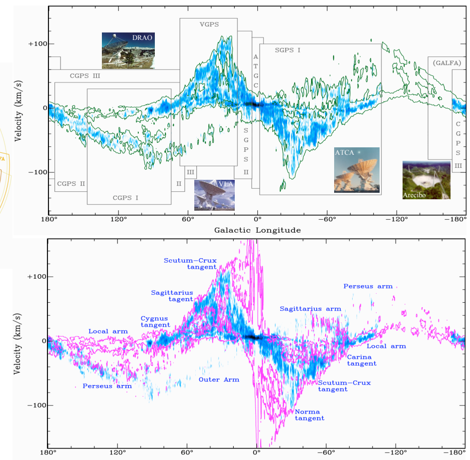

Figure 3. Using the HISA identification and extraction algorithms of Gibson et al. (2005b), we have mapped widespread HISA in the CGPS, VGPS, SGPS, and ATGC (top; green contour is searchable area with sufficiently bright background H I emission). HISA traces spiral arms in the outer Galaxy and tangent points in the inner Galaxy, where arm structure is hard to distinguish (above). CfA CO (magenta; Dame et al. 2001) matches HISA poorly in the outer Galaxy and better in the inner Galaxy, although the latter may be illusory (see **Figure 4**).

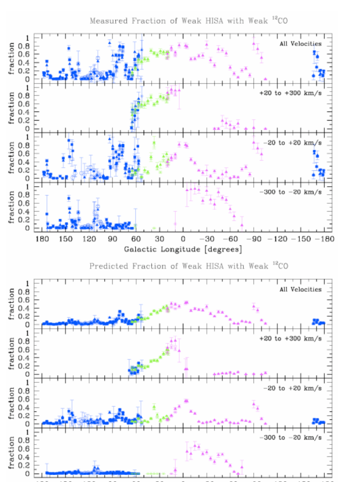

Figure 4. Fractions of HISA voxels (volume pixels) with CO emission at the same *(l,b,v)* position, and of CO voxels with HISA, measured for different survey data sets (see legend below) vs. longitude within different LSR velocity ranges to separate trends for local, inner-Galaxy, and outer-Galaxy gas. Symbols give the mean fraction and 1σ error in the mean within each 4°- or 5°-wide H I survey tile. *Upper left:* Apparent fraction of minimally-detectable HISA with minimally-detectable ^{12}CO, with $\Delta T_{b,HISA}$ < -15 K and $T_{b,12CO}$ > 1 K. *Middle left:* Predicted fraction if HISA and CO are unrelated physically and only align by chance, found as the product of the fraction of total voxels containing HISA and of that containing CO. This is more likely in the inner Galaxy where both HISA and CO are more abundant. *Bottom left:* "Corrected" fraction of HISA voxels with CO, found as the measured fraction minus the predicted fraction of random alignments. *Bottom row:* Corrected fractions also plotted for ^{12}CO with HISA, HISA with ^{13}CO, and ^{13}CO with HISA. Similar results are obtained for stronger-amplitude HISA and CO features (not shown), which display a somewhat greater affinity for each other.

Current Results

- Most HISA lacks CO emission at the same position and velocity. This is clear for HISA outside the Sun's orbit but is also likely for inner-Galaxy HISA if random alignments are removed. HISA must therefore arise from either unusually cold, isolated H I or trace H I inside CO-dark H_2 clouds.
- HISA with ^{13}CO is less common than HISA with ^{12}CO, probably because ^{13}CO is harder to detect than ^{12}CO.
- ^{13}CO with HISA is a little more common than ^{12}CO with HISA, perhaps indicating that HISA "prefers" cloud cores.
- CO with HISA is less common than HISA with CO, with a low enough fraction (< 10%) to raise concerns about the use of HISA to resolve near/far kinematic distance ambiguities in inner-Galaxy sight lines.

Future Work

- Rerun analysis using improved FCRAO CO data with "error beam" sidelobe contamination removed.
- Parallel analysis of HISA-CO spectral feature alignments and mean velocity separation; compare to voxel results.
- Incorporate GALFA survey HISA detections using augmented HISA identification algorithms under development.
- Incorporate additional HISA detections in subsequent surveys (e.g, GASKAP; Dickey et al. 2013).
- Compare empirical results to synthetic observations of rotating Galactic disk models.

Table 1: High-Resolution H I and CO Surveys Used in This Study

Survey	Line	Telescope	$\Delta\theta$	Δv	Plane Coverage, Total Area
CGPS[1]	H I 21 cm	DRAO-ST + 26 m	1′	0.8 km/s	$52° < \ell < 193°$, 1240 deg^2
VGPS[2]	H I 21 cm	VLA-D + GBT 100 m	1′	0.8 km/s	$18° < \ell < 67°$, 177 deg^2
SGPS[3]	H I 21 cm	ATCA + Parkes 64 m	2′	0.8 km/s	$253° < \ell < 20°$, 274 deg^2
ATGC[4]	H I 21 cm	ATCA + Parkes 64 m	2′	0.8 km/s	$355° < \ell < 5°$, 100 deg^2
GALFA[5]	H I 21 cm	Arecibo 305 m	4′	0.2 km/s	$31° < \ell < 77°, 169° < \ell < 214°$, $-1 < \delta < +38°$, 13,000 deg^2
OGS[6]	^{12}CO 2.6 mm	FCRAO 14 m	1′	0.8 km/s	$103° < \ell < 142°$, 328 deg^2
GRS[7]	^{13}CO 2.7 mm	FCRAO 14 m	1′	0.2 km/s	$14° < \ell < 56°$, 83 deg^2
EOGS[8]	^{12}CO + ^{13}CO	FCRAO 14 m	1′	0.2 km/s	$56° < \ell < 192°$, 820 deg^2
UMSB[6]	^{12}CO 2.6 mm	FCRAO 14 m	6′	1.0 km/s	$8° < \ell < 90°$, 164 deg^2
CfA[10]	^{12}CO 2.6 mm	CfA 1.2 m, N + S	9′	0.6 km/s	$0° < \ell < 360°$, 11,000 deg^2

[1]CGPS: Taylor et al. (2003); [2]VGPS: Stil et al. (2006); [3]SGPS: McClure-Griffiths et al. (2005)
[4]ATCA-GC: McClure-Griffiths et al. (2012); [5]GALFA-H I: Peek et al. (2011), Gibson et al. (2012; I-GALFA);
[6]OGS: Heyer et al. (1998); [7]GRS: Jackson et al. (2006); [8]EOGS: Brunt et al. (in prep; several areas)
[9]UMSB: Sanders et al. (1986); [10]CfA: Dame et al. (2001; multi-survey composite)

References

Dame, T. M., et al. 2001, ApJ, 547, 792
Dickey, J. M., et al. 2013, PASP, 30, 3
Gibson, S. J. 2010, ASPC, 438, 111
Gibson. S. J., et al. 2012, AAS, 219, 349.29
Gibson, S. J., et al. 2005b, ApJ 626, 195
Gibson, S. J., et al. 2005a, ApJ 626, 214
Gibson, S. J., et al. 2000, ApJ, 540, 851
Heyer, M. H., et al. 1998, ApJS, 115, 241
Jackson, J. M., et al. 2006, ApJS, 163, 145
McClure-Griffiths, N. M., et al. 2012, ApJS, 199, 12
McClure-Griffiths, N. M., et al. 2005, ApJS, 158, 178
Peek, J. E. G., et al. 2011, ApJS, 194, 20
Sanders, D. B., et al. 1986, ApJS, 60, 1
Stil, J. M., et al. 2006, 132, 1158
Taylor, A. R., et al. 2003, AJ, 125, 3145
Taylor, J. H., & Cordes, J. M. 1993, ApJ, 411, 674
Wolfire, M. G., et al. 2010, ApJ, 716, 1191
Wolfire, M. G., et al. 2003, ApJ, 587, 278

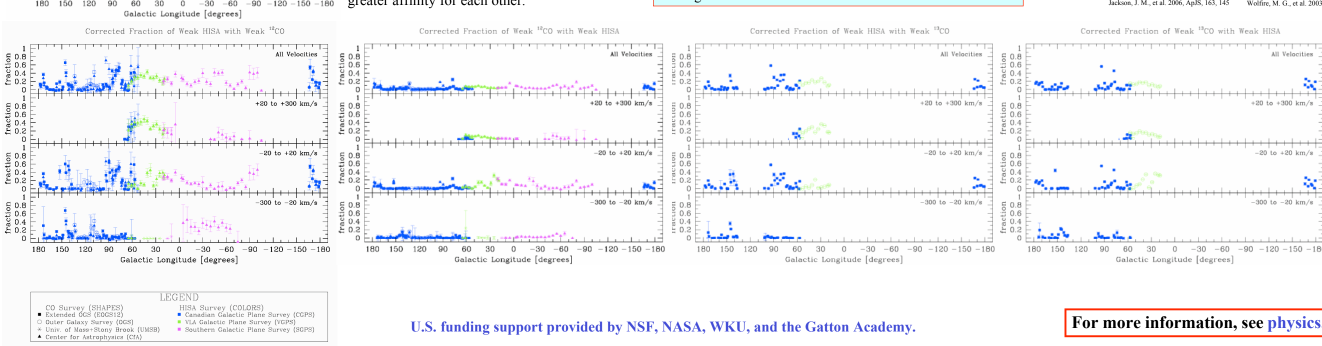

U.S. funding support provided by NSF, NASA, WKU, and the Gatton Academy.

For more information, see physics.wku.edu/~gibson